Near-infrared Spectroscopy of 3:1 Kirkwood Gap Asteroids (660) Crescentia, (797) Montana, (879) Ricarda, (1391) Carelia, and (1644) Rafita. S. K. Fieber-Beyer[1,2], M. J. Gaffey[1,2], and J.R. Blagen[1,2]. [1]Dept of Space Studies, Box 9008, Univ. of North Dakota, Grand Forks, ND 58202. [2]Visiting astronomer at the IRTF under contract from the NASA, which is operated by the Univ. of Hawai'i Mauna Kea, HI 96720. sherryfieb@hotmail.com

Introduction: The Kirkwood Gaps (KG) are depleted zones in the asteroid belt located at proper motion resonances with Jupiter. Theoretical models indicate the majority of asteroidal material delivered to the inner solar system, particularly to the Earth, originates from the 3:1 and ν_6 resonances [1-4].

The results of the Fragment Injection Model [1] were used to select asteroids predicted to be strong sources of meteoroids in Earth-crossing orbits. Asteroids with i >30° were not selected due to high geocentric velocities.

Probable parent bodies have been identified for four [5-7] of the 135 distinguishable meteorite classes [8]. These three parent bodies: 4 Vesta, 3103 Egar, and 6 Hebe account for ~40% of terrestrial meteorite falls. Therefore ~60% of the meteorite fall flux and ~97% of the meteorite classes still need to be accounted for. Asteroids within the "feeding zone" of the 3:1 KG are good candidates for such parent bodies.

Previous VNIR (~0.3 – 0.95 μm) spectral observations [9-13] of 3:1 KG asteroids do not permit the detailed mineralogical analysis required to rigorously test possible meteorite affinities. Ambiguities introduced by space weathering undermine the validity of any putative asteroid-meteorite links derived from curve matching, requiring the use of interpretive methodologies insensitive to space weathering [14].

Near-infrared spectral data in the 0.8-2.5 μm wavelength range is necessary for detailed characterizations of surface minerals and is not available for most asteroids adjacent to the 3:1 KG. By identifying the source asteroids of particular meteorite types, the asteroid "map" and meteorite "clock" can be combined to provide a much more sophisticated understanding of the history and evolution of the late solar nebula and the early solar system.

Thus far, the current research project has been successful in linking several asteroids to meteorite types such as the mesosiderites, H & LL-chondrites, CV/CO chondrites, pallasites/olivine bearing, & winonaite meteorites [15-17]. We continue to explore links between asteroids located near the 3:1 KG and potential meteorite analogs in the terrestrial collections.

Observations & Data Reduction: NIR spectra of asteroids (660), (797), (879), (1391), & (1644) were taken June 12 & 13, 2010 at the NASA IRTF using the SpeX instrument [18] in the low-res spectrographic mode. Asteroid & standard star observations were interspersed within the same airmass range to allow modeling of atmospheric extinction. Data reduction was done using previously outlined procedures [19,20].

The spectrum of each asteroid exhibits absorption features located near 1- and 2- μm (Fig. 1) with varying spectral redness. The band centers and band area ratios (BAR) are diagnostic of abundance and composition of the mafic silicates [e.g.,19-28] and are measured relative to a linear continuum fit tangent to the spectral curve outside the absorption feature [e.g. 23]. To estimate the error, several polynomial fits were used sampling different ranges of points within the Band I & II spectral intervals. The uncertainty was estimated from the difference between the minimum and maximum determined values (Table 1).

Analysis: Band Centers are plotted on Figure 2 [21,29]. Asteroids (797), (879), (1391), & (1644) plot within or very close to the HED Zone. On the S-Asteroid Subtype plot [24] the plotted parameters indicate assemblages containing abundant orthopyroxene (Fig. 3). The compositions of the surficial average pyroxene were calculated using equations outlined by [19]. The calculated pyroxene chemistries are consistent with pyroxenes in the HED meteorite group. Since ~80% of the meteorite parent bodies are differentiated [8], it isn't unreasonable to see so many achondrite assemblages. The weak absorption features suggest additional phases are affecting the band intensities (e.g. metal, feldspar, opaques, space weathering).

Asteroids (660) and (879) are part of the dynamical Maria Family [30]. The measured parameters of (879) are consistent with previous mineralogical interpretations of the Maria Family [16], which indicate silicate assemblages analogous to HED meteorites with an abundant NiFe metal phase, analogous to the mesosiderite meteorites. Asteroid (660) appears to be an interloper, with a spectrum indicative of spinel, similar to the spinel-bearing *CAI*s (calcium-aluminum inclusions) in the meteorite *Allende* [31,32]. The spectral contribution of spinel is much more pronounced in (660) than in previously identified spinel-bearing asteroids [17] (Fig. 4).

Conclusions: Spectra of asteroids (797), (879), (1391), & (1644) indicate assemblages spectrally dominated by pyroxene. These objects are currently being analyzed for possible meteorite analogs (excluding (879)). Asteroid (660) is a spinel-bearing asteroid with

a surface concentration much greater than any other spinel-bearing asteroid to date.

References: [1] P. Farinella et al. (1993) *Icarus* 101, 174-187. [2] A. Morbidelli et al. (1995) *Icarus* 114, 33-50. [3] A. Morbidelli et al. (1995) *Icarus* 115,60-65. [4] J.H. Ji et al. (2007) *Chin. J. Astron. Astrophys* **7**, 148-54. [5] T.B. McCord et al. (1970) *Science* 168, 1445-47. [6] M.J. Gaffey et al. (1992) *Icarus* 100, 95-109. [7] M.J. Gaffey et al. (1998) MAPS 33, 1281-95. [8] K. Keil (2000) *Planet. Space Sci.* 48, 887-903. [9] L.A. McFadden et al. (1984) *Icarus* 59, 25-40. [10] L.A. McFadden et al. (1987) *Lunar Planet. Sci. XVIII*, 614-15. [11] L.A. McFadden et al. (1991) *Asteroids, Comets, Meteors* 416-23. [12] F. Vilas et al. (1992) *Icarus* 100, 85-94. [13] C.R. Chapman et al. (1979) Univ. of Arizona Press, Tucson, 655-87. [14] M.J. Gaffey (2010) *Icarus* 209, 564-74. [15] S.K. Fieber-Beyer et al. (2011) *Icarus* 212, 149-57. [16] S.K. Fieber-Beyer et al. (2011) *Icarus* 213, 524-37. [17] S.K. Fieber-Beyer et al. (2011) *Icarus* 214, 645-51. [18] J.T. Rayner et al. (2003) *Pubs. of the Astronomical Society of the Pacific* 115, 362-82. [19] M.J. Gaffey et al. (2002), *Asteroids III*, 183-204. [20] P.S. Hardersen et al. (2005) *Icarus* 175, 141-58. [21] J.B. Adams (1974) *JG R*79, 4829-36. [22] J.B. Adams (1975) *In Infrared and Raman Spectroscopy of Lunar and Terrestrial Minerals,* 91-116. [23] E.A. Cloutis et al. (1986) *JGR* 91, 11641-53. [24] M.J. Gaffey et al. (1993) *Icarus* 106, 573-602. [25] H.K. Gastineau-Lyons et al. (2002) *MAPS* 37, 75-89. [26] T.H. Burbine et al. (2003) *Antarct. Meteorite Res.* 16, 185-95. [27] T.H. Burbine et al. (2009) *MAPS.* 44, 1331–41. [28] T.L. Dunn et al. (2010) *Icarus 208, 789–97*. [29] E.A. Cloutis et al. (1991) *JGR* 96, 22809-826. [30] V. Zappalà et al. (1995) *Icarus* 116, 291-314. [31] S. Rajan et al. (1984) Lunar Planet. Sci. 15, 284–85. [32] J.M. Sunshine et al. (2008) *Science* 320, 514–17.

Acknowledgements: This work was supported by NASA NESSF Grant NNX08AW0414 (SKF-B) and NASA PGG Program Grant NNX07AP73G (MJG).

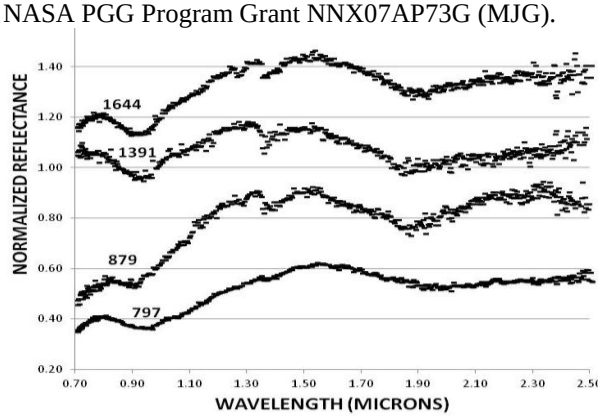

Figure 1

Table 1

	660	797	879	1391	1644
Band I (μm)	NA	0.95±.02	0.92± .01	0.93 ± .02	0.93 ± .01
Band II(μm)	NA	1.98±.02	1.87± .03	2.00± .05	1.89 ± .02
BAR	NA	1.61±.10	2.56± .30	2.31± .34	1.74 ± .10
Pyx Comp	NA	$Fs_{41\ (\pm5)}$ $Wo_{15\ (\pm4)}$	$Fs_{18\ (\pm5)}$ $Wo_{3\ (\pm3)}$	$Fs_{53\ (\pm5)}$ $Wo_{9\ (\pm4)}$	$Fs_{23(\pm5)}$ $Wo_{6\ (\pm3)}$

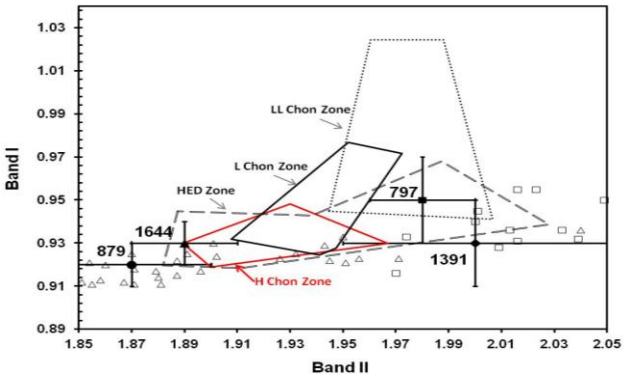

Figure 2

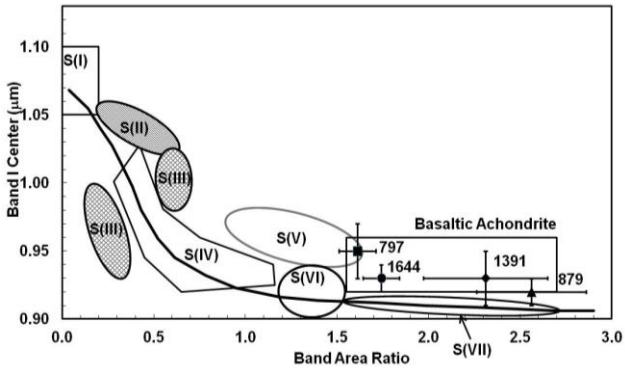

Figure 3

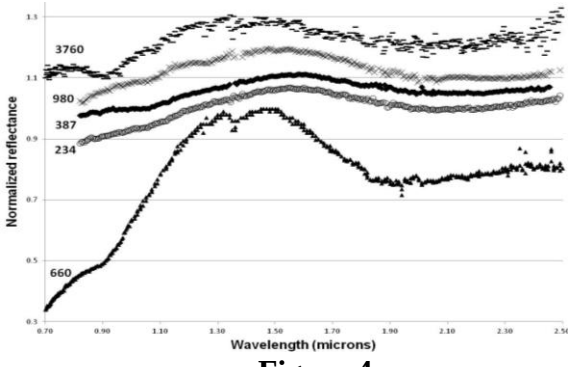

Figure 4